

# Non- $\Phi_0$ -periodic macroscopic quantum interference in one-dimensional parallel Josephson junction arrays with unconventional grating structure

J. Oppenländer, Ch. Häussler, and N. Schopohl

*Institut für Theoretische Physik, Eberhard-Karls-Universität Tübingen, Auf der Morgenstelle 14, D-72076 Tübingen, Germany*

(Received 1 August 2000; published 20 December 2000)

A theoretical study is presented for a number  $N$  of Josephson junctions connected as a one-dimensional (1D) parallel array in such a manner that there are  $N-1$  individual superconducting loops with arbitrary shape formed. In the resistive array mode, for bias currents  $I > I_c$ , all Josephson junctions in the array oscillate at the same magnetic field dependent frequency  $\nu_B$  which is, in general, *not* a  $\Phi_0$ -periodic function of the strength of magnetic field  $\mathbf{B}$ . Within the range of validity of the resistively and capacitively shunted junction (RCSJ) model the periodicity of  $\nu_B$  is controlled by the array geometry alone and does not depend on the distribution of the array junction parameters. In the overdamped junction regime,  $\nu_B$  is for certain types of *unconventional grating structures* a *unique* function around a sharp *global* minimum at  $\mathbf{B}=0$ . This *filter property* does not apply for regular gratings and superconducting quantum interference devices (SQUID's). Computer simulations of the full nonlinear array dynamics reveal that the qualitative macroscopic quantum interference properties of unconventional arrays are governed, irrespective of the strength of inductive couplings, by a complex structure factor  $S_N(\mathbf{B})$  which can be determined analytically. Also, the performance of magnetometers based on 1D arrays with unconventional grating structure can be significantly better than the performance of conventional SQUID's. In particular, 1D arrays with unconventional grating structure should provide a technically rather unsophisticated precision measurement of *absolute* strength and orientation of external magnetic fields.

DOI: 10.1103/PhysRevB.63.024511

PACS number(s): 85.25.Dq, 85.25.Am, 85.25.Cp

## I. INTRODUCTION

So-called weak links, or Josephson junctions, are the basic active elements of superconductor quantum electronics. A key feature of a weak link between two superconductors, 1 and 2, is the property that there can flow a dissipationless macroscopic supercurrent  $I_s(\varphi)$  due to the tunneling of Cooper pairs<sup>1</sup> with charge  $2e$ . This supercurrent depends on the gauge invariant phase difference  $\varphi = \Theta_1 - \Theta_2 + (2e/\hbar) \int_1^2 \langle d\mathbf{s}, \mathbf{A} \rangle$  of the macroscopic BCS pairing wave functions on either side of the weak link. Josephson junctions made with modern fabrication techniques<sup>2</sup> often have a sandwich type layered geometry, with a thin nonsuperconducting tunneling barrier in the middle between two thick superconducting electrodes. In recent time also other types of weak links, for example, of the bicrystal type, became important in high-temperature superconductors.<sup>3,4</sup> For an ideal  $S$ - $I$ - $S$  junction the supercurrent is connected to the phase difference  $\varphi$  across the tunneling barrier by  $I_s(\varphi) = I_c \sin \varphi$ . The supercurrent  $I_s$  flows stationary provided it does not exceed a characteristic critical current  $I_c$ , the so-called Josephson critical current, which determines the maximum dissipationless current that can flow across a tunneling barrier. In general,  $I_c$  depends on the material properties of the junction, on temperature  $T$ , and also on magnetic field  $\mathbf{B} = \text{rot } \mathbf{A}$ . Applying to a Josephson junction a bias current  $I$  with a constant strength  $I > I_c$ , there appears a rapidly oscillating voltage signal  $V(t)$  across the junction, which determines the rate of change of the time dependent phase difference  $\varphi(t)$  according to

$$\hbar \partial_t \varphi(t) = 2eV(t). \quad (1)$$

This is the fundamental nonstationary Josephson relation which governs the physics of weak superconductivity.<sup>1</sup> For  $I > I_c$  there flows, in addition to the dissipationless supercurrent  $I_s$ , also a dissipative normal current  $I_n$  in the junction, whose physical origin is the transfer of single (unpaired) electrons.

Within the range of validity of the RCSJ model,<sup>5</sup> the dissipative current may be described with sufficient accuracy as a superposition of an ohmic current, characterized by a parallel ohmic shunt resistance  $R$ , and a displacement current, which is characterized by a parallel geometric shunting capacitance  $C$  describing electric polarization inside the tunneling barrier. The total junction current  $I$  is then

$$I = I_c \sin \varphi(t) + \frac{\hbar}{2eR} \partial_t \varphi(t) + \frac{\hbar C}{2e} \partial_t^2 \varphi(t). \quad (2)$$

The time average

$$\langle V \rangle = \lim_{t \rightarrow \infty} \frac{1}{t} \int_0^t dt' V(t') = \frac{\hbar}{2e} \lim_{t \rightarrow \infty} \frac{\varphi(t) - \varphi(0)}{t} \quad (3)$$

is the dc voltage part of the, in general, not sinusoidal voltage signal  $V(t)$  across the electrodes of a Josephson junction. For a strongly overdamped junction,  $C=0$ , one finds, assuming a constant bias current  $I > I_c$ , a relatively simple formula<sup>5</sup>  $\langle V \rangle = R \sqrt{I^2 - I_c^2}$ .

The dc voltage  $\langle V \rangle$  is connected to the oscillation frequency  $\omega = 2\pi\nu$  of the voltage signal  $V(t)$  by

$$h\nu = 2e\langle V \rangle. \quad (4)$$

This result for the voltage response function  $\langle V \rangle$  of a weak link suggests a spectroscopic interpretation. When a Cooper pair is transferred from the superconducting side 1 to the

superconducting side 2 of the junction, under conditions where  $I > I_c$ , a microwave photon with energy  $2e\langle V \rangle$  is released in the form of one quantum of electromagnetic radiation (Josephson radiation<sup>6</sup>).

As far as macroscopic quantum interference is concerned, it was actually known<sup>7</sup> long before the discovery of the Josephson effects, that magnetic flux threading the area of a superconducting ring, made out of a material that is thick compared to the magnetic penetration depth  $\lambda$ , should be quantized in units of the flux quantum  $\Phi_0 = h/2e$ . This is a consequence of a theoretical argument first employed by Onsager<sup>8</sup> in the context of the quantization of circulation in superfluid <sup>4</sup>He. The macroscopic wave function of particles moving round a closed loop displays necessarily an integer multiple of wavelengths over the full length of a closed orbit. So, the electric current circulating in such a superconducting ring is quantized, which in turn implies the quantization of the total magnetic flux threading the area of that ring.<sup>7</sup> Technical applications of the physics of weak superconductivity<sup>5,9</sup> include ultrasensitive quantum interferometers, which indeed combine the aforementioned Josephson effects with flux quantization.

In this paper we investigate macroscopic quantum interference phenomena in one-dimensional (1D) parallel arrays of Josephson junctions with unconventional grating structure, i.e., multiple-loop configurations that are characterized by an intrinsic nonperiodicity of the geometry of the structure. For such multiple-loop configurations the interference effects are generated by the phase-sensitive<sup>10</sup> superposition of a mesoscopic number of macroscopic array junction currents in the presence of an external magnetic field. The Josephson junctions in the array are required to be *short* junctions such that any spatial variations of the gauge invariant phase differences along the barriers of the weak links can be safely neglected. Then the array junctions are well described by the RCSJ model as stated in Eq. (2) which provides, e.g., a successful description for resistively shunted low- $T_c$  junctions or high- $T_c$  bicrystal junctions.<sup>4</sup> The use of *short* junctions ensures that the nonlinear array dynamics is dominated by the collective effects we want to study and not by the intrinsic dynamics of the individual junctions.

In Sec. II we briefly summarize the basic properties of standard single loop two-junction superconducting quantum interference devices (SQUID's) and periodic multiple loop parallel 1D arrays, i.e., geometrical configurations with conventional grating structures. In Sec. III we focus on the basic properties of *unconventional* grating structures. Then, in Sec. IV, we present a unified theoretical description of general 1D parallel arrays, and we discuss analytical as well as numerical results. In Sec. V we briefly discuss the noise properties of unconventional arrays. Finally, Sec. VI is devoted to the discussion of our results and future perspectives.

## II. CONVENTIONAL GRATING STRUCTURES

Consider, as indicated schematically in Fig. 1(a), a standard two junction SQUID (for simplicity with symmetric junction parameters) under the dc current bias  $I > 2I_c$ . Such a device is actually a flux-to-voltage transducer.<sup>5</sup> Let  $\Phi$

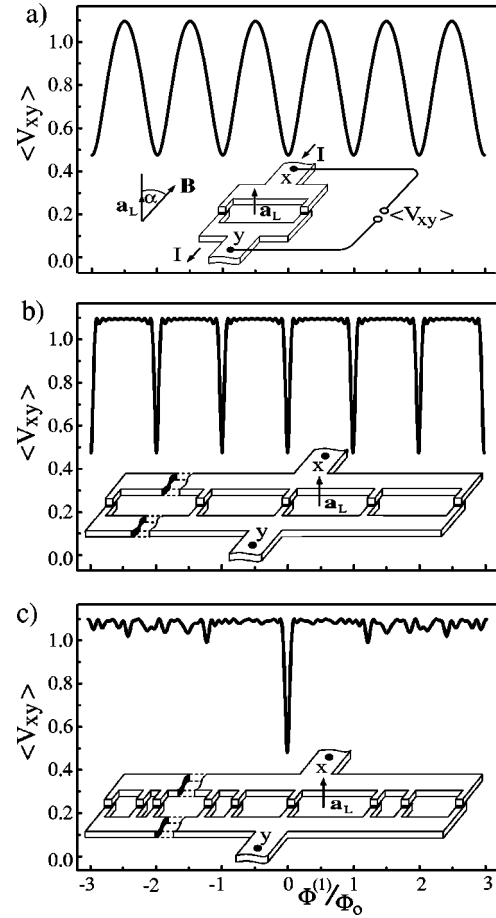


FIG. 1. Voltage response  $\langle V_{xy} \rangle$  in units of  $I_c R$  vs external flux  $\Phi^{(1)}$  through largest area element  $\mathbf{a}_L$  of interferometer with  $N$  (overdamped) junctions for bias current  $I = 1.1 NI_c$  and vanishing inductive coupling: (a) symmetrical SQUID ( $N=2$ ), (b) periodic 1D array ( $N=11$ ), (c) 1D array with unconventional grating structure ( $N=18$ ). The loop areas in (c) are randomly distributed between 0.1 and  $1.0|\mathbf{a}_L|$  but with same total area as in (b).

$=\langle \mathbf{B}, \mathbf{a} \rangle = |\mathbf{B}| |\mathbf{a}| \cos \alpha$  be the magnetic flux threading the orientated area element  $\mathbf{a}$  of the superconducting SQUID loop, where  $\alpha$  is the angle between the normal vector of the orientated area element and the magnetic field vector  $\mathbf{B}$ , as depicted schematically in Fig. 1(a). The total magnetic field  $\mathbf{B} = \mathbf{B}^{(1)} + \mathbf{B}^{(2)}$  is then a superposition of the *primary* external magnetic field  $\mathbf{B}^{(1)}$ , which generates the flux  $\Phi^{(1)} = \langle \mathbf{B}^{(1)}, \mathbf{a} \rangle$  one wants to detect, and a *secondary* magnetic field  $\mathbf{B}^{(2)}$  that results from the screening current  $I_{sc}$  circulating in the SQUID loop. The total flux in the loop is given by  $\Phi = \Phi^{(1)} + \Phi^{(2)}$ , with  $\Phi^{(2)} = -LI_{sc}$  where  $L$  denotes the inductance of the loop. Depending on the secondary flux term  $\Phi^{(2)}$  there exists an optimal size  $|\mathbf{a}_L|$  for any SQUID loop if the parameters are optimized with respect to the sensitivity of the device.<sup>4,9</sup> A dimensionless measure for the inductance of a single loop is  $\beta_L = LI_c / \Phi_0$ . The voltage response function  $\langle V_{xy} \rangle$  of the SQUID, i.e., the time average of the rapidly oscillating voltage signal  $V_{xy}(t)$  across the nodes  $x$  and  $y$  of the circuit, is a  $\Phi_0$ -periodic function of the strength of external magnetic field, see Fig. 1(a). Therefore, a *two* junction

SQUID cannot be directly employed as a detector of *absolute* strength of external magnetic field.

A straightforward extension of the standard two junction SQUID is sketched in Fig. 1(b). This is a 1D array of  $N$  adjacent Josephson junctions connected in parallel.<sup>5,11</sup> The area elements of the  $N-1$  SQUID loops are all equal, i.e.,  $\mathbf{a}_n = \mathbf{a}_L$  for all  $n$ . The voltage response signal  $\langle V_{xy} \rangle$  vs strength  $|\mathbf{B}^{(1)}|$  of external magnetic field of such a *periodic* array has the same period  $\Phi_0$  than a standard two junction SQUID with loop area  $|\mathbf{a}_L|$ , see Fig. 1(b). Such a device, therefore, can also not be used as a detector of *absolute* strength of magnetic field.

### III. UNCONVENTIONAL GRATING STRUCTURES

A more general quantum interference device is obtained when the area elements  $\mathbf{a}_n$  of the  $N-1$  loops in the array differ in size and, possibly, in orientation, as depicted schematically in Fig. 1(c). If the sizes  $|\mathbf{a}_n|$  of the orientated area elements  $\mathbf{a}_n$  of the individual superconducting loops are chosen in such a way that for a finite external magnetic field  $\mathbf{B}^{(1)}$  a coherent superposition of the array junction currents (see Sec. IV) is prevented, the voltage response function  $\langle V_{xy} \rangle$  vs  $|\mathbf{B}^{(1)}|$  becomes nonperiodic. From the analogy to optical interference patterns we call such configurations unconventional grating structures.

An example for the effects of unconventional grating on the voltage response function is shown in Fig. 1(c). The areas of the different array loops are chosen randomly between  $0.1|\mathbf{a}_L|$  and  $1.0|\mathbf{a}_L|$ , while the total area of the array is the same as for the periodic array, Fig. 1(b). The maximum loop size coincides with the corresponding optimal loop size of a standard two junction SQUID, i.e.,  $\max|\mathbf{a}_n| = |\mathbf{a}_L|$ . By this, the response function of the unconventional array shown in Fig. 1(c) is comparable to the response functions shown in Figs. 1(a) and 1(b).

The distribution of the array loop sizes has two properties that prevent for a finite external magnetic field  $\mathbf{B}^{(1)}$  the coherent superposition of the array junction currents. First, **the loop sizes are incommensurable, i.e., there exists no greatest common divisor (GCD).** Second, **the size of the smallest loop  $|\mathbf{a}_{\min}|$  strongly differs from the size of the largest loop  $|\mathbf{a}_{\max}|$ , and the sizes of all other loops are distributed between  $|\mathbf{a}_{\min}|$  and  $|\mathbf{a}_{\max}|$  in such a way that no distinct loop size is preferred.** The first property of the distribution prevents any (strong) periodicity of the response function. The second property ensures that no significant partially coherent superposition of the array junction currents takes place, i.e., that there exist no finite values of  $\mathbf{B}^{(1)}$  for which additional significant antipeaks in the voltage response function do occur. If these two necessary conditions are fulfilled by the loop size distribution, the voltage response signal  $\langle V_{xy} \rangle$  vs strength of magnetic field of the unconventional junction array becomes, under a suitable dc current bias  $I$ , a unique function of  $|\mathbf{B}^{(1)}|$  around its narrow global minimum at  $|\mathbf{B}^{(1)}| = 0$ . This feature of the voltage response function of unconventional arrays does only depend on the distribution of the array loop sizes. It does not depend on parameter

spreads in the parameters of the individual array junctions (see Sec. IV).

In contrast to devices with conventional grating structures, the uniqueness of the voltage response function of unconventional arrays allows such devices to be directly employed as **detectors of absolute strength of external magnetic field.** It should be possible, e.g., by measuring control current(s) flowing through the wires of a set of suitably orientated compensation coil(s), to reconstruct *absolute* strength, orientation and even the phase of an incident primary magnetic field signal, i.e., to determine the full vector  $\mathbf{B}^{(1)}(t)$ .

### IV. UNIFIED THEORETICAL DESCRIPTION OF 1D PARALLEL JOSEPHSON JUNCTION ARRAYS

The  $n$ th Josephson junction in the array has, within the range of validity of the RCSJ model, optional individual junction parameters  $R_n$ ,  $C_n$ , and  $I_{c,n}$ . The corresponding current  $I_n$  flowing through the  $n$ th Josephson junction is, according to Eq. (2), determined by the gauge invariant phase difference  $\varphi_n(t)$  across that junction. The total current  $I$  flowing through the nodes  $x$  and  $y$ , respectively, of the circuit is then obtained from Kirchhoff's rule as the *phase sensitive* superposition of the individual junction currents  $I_n$

$$I = \sum_{n=1}^N \left[ I_{c,n} \sin \varphi_n(t) + \left( \frac{\hbar C_n}{2e} \partial_t^2 + \frac{\hbar}{2e R_n} \partial_t \right) \varphi_n(t) \right]. \quad (5)$$

The gauge invariant phase differences  $\varphi_n$  of adjacent Josephson junctions in the array are not independent, but are connected to each other by the condition of flux quantization

$$\varphi_{n+1} - \varphi_n = \frac{2\pi}{\Phi_0} \langle \mathbf{B}, \mathbf{a}_n \rangle \bmod 2\pi. \quad (6)$$

Here  $|\mathbf{a}_n|$  is the area of the superconducting loop connecting adjacent Josephson junctions numbered as  $n$  and  $n+1$ , respectively, and  $\mathbf{B}$  denotes the magnetic field threading the orientated area element  $\mathbf{a}_n$  of this loop. Equation (6) applies quite generally, provided the superconducting material, out of which the connecting loops are made, is thick compared to the magnetic penetration depth  $\lambda$ . In this case there exists a path inside the wire connecting, say, junction  $n$  with its neighbor junction  $n+1$ , on which the superfluid velocity field  $\mathbf{v}_s$  becomes negligibly small. So,  $\hbar \nabla \Theta = 2e \mathbf{A}$  along this path.

Since all junctions in the array are connected in parallel, the rapidly oscillating voltage  $V_n(t)$  at the electrodes of a particular Josephson junction, numbered as  $n$  in the array, is related to the signal  $V_{xy}(t)$  between the nodes  $x$  and  $y$  of the circuit by

$$V_{xy}(t) = V_n(t) + \int_{x \rightarrow n \rightarrow y} \langle d\mathbf{s}, \mathbf{E}(t) \rangle. \quad (7)$$

By Faraday's law the electric field  $\mathbf{E}$  along an integration path  $x \rightarrow n \rightarrow y$ , that starts at node  $x$ , traverses the tunneling barrier of the  $n$ th Josephson junction just once, and then terminates at node  $y$ , is directly connected to the time deriva-

tive of the flux threading the area elements of the 1D array. Once the signal  $V_1(t) = (\hbar/2e)\partial_t\varphi_1(t)$  is known the other voltage signals  $V_n(t)$  across the electrodes of the  $n$ th junction follow from

$$V_{n+1}(t) - V_n(t) = \partial_t \langle \mathbf{B}(t), \mathbf{a}_n \rangle. \quad (8)$$

Taking into account the Biot-Savart type inductive couplings<sup>12,13</sup> among the currents flowing in the circuit prohibits further simplification. However, in the limit of vanishing inductance the problem can be treated analytically. This will be done in the following Sec. IV A. The full problem, for arbitrary inductive couplings, will then be discussed in Sec. IV B.

### A. 1D parallel arrays with vanishing inductance

If all array loop inductance parameters  $\beta_{L_n}$  are small, i.e.,  $\beta_{L_n} \ll 1$  for all  $n=1, \dots, N-1$ , the currents flowing in the array do not generate a significant secondary magnetic field  $\mathbf{B}^{(2)}$ . In this limit of vanishing array inductances  $\mathbf{B} = \mathbf{B}^{(1)}$  holds. Then it follows directly from Eq. (6) that one can eliminate from Eq. (5) all phase variables  $\varphi_n(t)$  in favor of a single phase variable, say  $\phi(t) = \varphi_1(t)$ . In this case the problem of  $N$  coupled Josephson junctions is mapped onto a virtual *single* Josephson junction model. With  $\phi(t) = \varphi_1(t)$  and

$$I_c = \frac{1}{N} \sum_{n=1}^N I_{c,n}, \quad (9a)$$

$$\frac{1}{R} = \frac{1}{N} \sum_{n=1}^N \frac{1}{R_n}, \quad (9b)$$

$$C = \frac{1}{N} \sum_{n=1}^N C_n, \quad (9c)$$

$$T_N = \frac{\hbar}{2e} \frac{1}{I_c R}, \quad (9d)$$

$$J_N = \frac{I}{N I_c}, \quad (9e)$$

there results a *scalar* differential equation determining the phase difference  $\phi(t)$ :

$$\begin{aligned} & |S_N(\mathbf{B})| \sin[\phi(t) + \delta_N(\mathbf{B})] + T_N(RC \partial_t^2 + \partial_t) \phi(t) \\ & = J_N - \frac{2\pi}{\Phi_0} T_N(RC \partial_t^2 \langle \mathbf{B}, \mathbf{a}_C \rangle + \partial_t \langle \mathbf{B}, \mathbf{a}_R \rangle). \end{aligned} \quad (10)$$

Here we have introduced the definitions

$$S_N(\mathbf{B}) = \frac{1}{N} \sum_{n=1}^N \frac{I_{c,n}}{I_c} \exp\left[\frac{2\pi i}{\Phi_0} \sum_{m=0}^{n-1} \langle \mathbf{B}, \mathbf{a}_m \rangle\right], \quad (11)$$

and

$$\mathbf{a}_R = \frac{1}{N} \sum_{n=1}^N \frac{R}{R_n} \sum_{m=0}^{n-1} \mathbf{a}_m, \quad (12a)$$

$$\mathbf{a}_C = \frac{1}{N} \sum_{n=1}^N \frac{C_n}{C} \sum_{m=0}^{n-1} \mathbf{a}_m, \quad (12b)$$

$$\mathbf{a}_0 = \mathbf{0}. \quad (12c)$$

The complex function  $S_N(\mathbf{B}) = |S_N(\mathbf{B})| e^{i\delta_N(\mathbf{B})}$ , as defined in Eq. (11), denotes the characteristic *structure factor* of the 1D parallel Josephson junction array. It is an extremely responsive function of strength and orientation of magnetic field  $\mathbf{B}$ , and it is strongly affected by the choice of the individual area elements  $\mathbf{a}_m$ . In general,  $|S_N(\mathbf{B})|$  is also very sensitive to permutations among the  $\mathbf{a}_m$ 's.

In the overdamped junction regime,  $C=0$ , under conditions where a constant current  $I$  is biased such that  $1 \geq |S_N(\mathbf{B})|/J_N \equiv \sin \alpha_B$ , and assuming for simplicity a homogeneous static magnetic field  $\mathbf{B}$  (as well as time independent area elements  $\mathbf{a}_m$ ), one finds an exact solution of Eq. (10) for the phase difference  $\phi(t)$ :

$$V_1(t) = \frac{\hbar}{2e} \partial_t \phi(t) = I_c R \frac{J_N^2 - |S_N(\mathbf{B})|^2}{J_N + |S_N(\mathbf{B})| \sin(\omega_B t - \alpha_B)}. \quad (13)$$

For a static magnetic field  $\mathbf{B}$  the voltage response function  $\langle V_{xy} \rangle$  measured between the nodes  $x$  and  $y$  of the circuit is equal to the dc part of the rapidly oscillating voltage signal  $V_1(t)$ . All Josephson junctions in the 1D array oscillate at the same frequency  $\omega_B = 2\pi \nu_B$ , which is related to  $\langle V_{xy} \rangle$  by

$$\frac{h}{2e} \nu_B = \langle V_1 \rangle = I_c R \sqrt{J_N^2 - |S_N(\mathbf{B})|^2} = \langle V_{xy} \rangle. \quad (14)$$

The oscillation frequency  $\nu_B$  of such a local oscillator is even more sensitive to changes of strength or orientation of the external magnetic field  $\mathbf{B}$  than the structure factor of the array itself, since  $|S_N(\mathbf{B})|$  enters into Eq. (14) quadratically. The Einstein-Planck relation determining the energy  $E$  of a radiated photon,  $E = h \nu_B$ , suggests then an analogy to an artificial atom with a tunable energy level distance  $E = 2e \langle V_{xy} \rangle$ .

For bias currents  $J_N \leq |S_N(\mathbf{B})|$  in the presence of static magnetic fields  $\mathbf{B}$ , Eq. (10) possesses a time-independent solution for which the voltage response  $V_1(t)$  vanishes. In this case, the magnetic field dependent critical current of the 1D parallel Josephson junction array is given by  $N I_c |S_N(\mathbf{B})|$ . So, the subcritical diffraction pattern of a parallel array consisting of  $N-1$  different loops with arbitrary shape is directly proportional to the modulus  $|S_N(\mathbf{B})|$  of the complex structure factor  $S_N(\mathbf{B})$ .

Consider, as in Sec. II, a periodic array, consisting of  $N-1$  identical SQUID loops, such that  $\langle \mathbf{B}, \mathbf{a}_n \rangle = \Phi = \langle \mathbf{B}, \mathbf{a}_L \rangle$ , and  $R_n = R, C_n = C, I_{c,n} = I_c$  independent on the junction index  $n$ . Then the structure factor  $S_N(\mathbf{B}) \equiv S_N^{(\Phi)}$  becomes a simple geometrical series

$$S_N^{(\Phi)} = \frac{\sin\left(\pi \frac{\Phi}{\Phi_0} N\right)}{N \sin\left(\pi \frac{\Phi}{\Phi_0}\right)} \exp\left[\pi i \frac{\Phi}{\Phi_0} (N-1)\right]. \quad (15)$$

Figure 1(b) shows the voltage response of a periodic array with  $N=11$  overdamped Josephson junctions according to Eq. (14). One observes the narrowing proportional to  $1/N$  of the width of the voltage response signal  $\langle V_{xy} \rangle$  around its minima. Note the periodicity property  $|S_N^{(\Phi+\Phi_0)}| = |S_N^{(\Phi)}|$  for all  $N \geq 2$ . For  $N=2$  Eq. (14) is the periodic voltage response of a symmetric two junction SQUID in the overdamped junction regime<sup>5</sup> [see Fig. 1(a)].

A structure factor with a much longer period is obtained in a parallel junction array where the orientated area elements increase in size according to a *linear* relation

$$\mathbf{a}_m = (2m-1)\mathbf{a}_1. \quad (16)$$

For simplicity, identical junction parameters  $R_n$ ,  $C_n$ , and  $I_{c,n}$  are assumed. Then

$$S_N(\mathbf{B}) = \frac{1}{N} \sum_{n=0}^{N-1} \exp\left[2\pi i \frac{\langle \mathbf{B}, \mathbf{a}_1 \rangle}{\Phi_0} n^2\right]. \quad (17)$$

The total area occupied by such a *Gaussian* array is  $\sum_{m=1}^{N-1} (2m-1)|\mathbf{a}_1| = (N-1)^2|\mathbf{a}_1|$ , where  $\mathbf{a}_1$  is the smallest area element, and  $\mathbf{a}_{N-1} = (2N-3)\mathbf{a}_1$  is the largest area element. The class of Gaussian arrays provides an interesting example of a nongeneric unconventional grating. Obviously, the first necessary property of a generic unconventional array is not fulfilled, because the loop area sizes  $|\mathbf{a}_m|$  of the array are commensurable. However, the second necessary property concerning the distribution of the area sizes is preserved (see Sec. III). Consequently, a Gaussian array displays a periodic voltage response, though, possibly, the period may become rather long. To determine the period of the Gaussian array consider a case where the flux threading the area of the smallest element  $\mathbf{a}_1$  is equal to a rational multiple of half a flux quantum:  $\langle \mathbf{B}, \mathbf{a}_1 \rangle = (M/N)(\Phi_0/2)$ . Then the largest area element in the array  $\mathbf{a}_{N-1}$ , is threaded by a flux  $\Phi_M = (1-3/2N)M\Phi_0$ . In this case the structure factor  $S_N(\mathbf{B}) \equiv S_N^{(\Phi_M)}$  may be determined using a result of Gauss<sup>14</sup>

$$S_N^{(\Phi_M)} = \frac{1}{N} \sum_{n=0}^{N-1} e^{\pi i (M/N)n^2} = \frac{e^{i(\pi/4)} M^{-1}}{\sqrt{NM}} \sum_{m=0}^{M-1} e^{-\pi i (N/M)m^2}. \quad (18)$$

Note the periodicity  $|S_N^{(\Phi_M+\Phi_{2N})}| = |S_N^{(\Phi_M)}|$ , with period  $\Phi_{2N} = (2N-3)\Phi_0$ . Remarkably, for  $M=2$ , and  $N=N_1N_2$  being the product of two prime numbers  $N_1$  and  $N_2$ , there holds the factorization

$$S_N^{(\Phi_2)} = (-1)^{(N_1-1)(N_2-1)/4} S_{N_1}^{(\Phi_2)} S_{N_2}^{(\Phi_2)}. \quad (19)$$

Apparently, such Gaussian arrays are governed by the laws of number theory (quadratic residues<sup>15</sup>).

Compare now a Gaussian array, with  $N-1$  area elements as described in Eq. (16), with a *periodic* array, consisting of

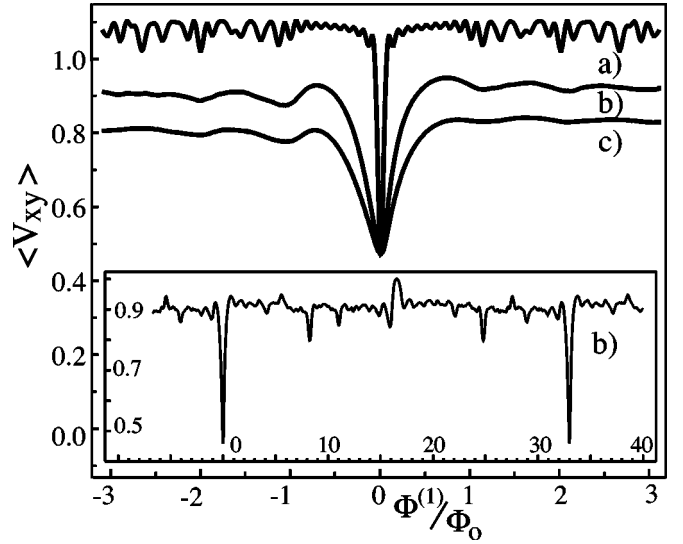


FIG. 2. Voltage response  $\langle V_{xy} \rangle$  in units of  $I_c R$  vs external flux  $\Phi^{(1)}$  through largest area element  $\mathbf{a}_L$  for a Gaussian array with  $N=18$  (overdamped) junctions for bias current  $I=1.1NI_c$  and various inductive couplings (a)  $\beta_L=0$ , (b)  $\beta_L=0.3$ , and (c)  $\beta_L=0.7$ .

$N_p-1$  identical SQUID loops with size  $|\mathbf{a}_L|$ . For a useful comparison, both arrays should occupy about the same total area:  $(N-1)^2|\mathbf{a}_1| = (N_p-1)\mathbf{a}_L$ . Also the largest area element in the Gaussian array should coincide with the area element of an optimal single SQUID loop, i.e.,  $\mathbf{a}_{N-1} = \mathbf{a}_L$ . Both requirements together imply for  $N_p \gg 1$  that the Gaussian array has the double number of junctions compared to a corresponding periodic junction array:  $N \approx 2N_p$ . Figure 2(a) shows the voltage response of a Gaussian array with  $N=18$  overdamped junctions as a function of the applied magnetic flux  $\Phi_M = \Phi^{(1)}$  through the largest area element according to Eq. (14). It differs substantially from the voltage response of the corresponding periodic array with identical loop areas as a comparison of Figs. 1(b) and Fig. 2(a) reveals. The voltage response of the Gaussian array possess a period  $(2N-3)$  times larger than the voltage response of the corresponding periodic array, while the steepness of the voltage transfer function  $V_\Phi = \partial \langle V \rangle / \partial \Phi^{(1)}$  around the remaining antipeaks is preserved [see Fig. 2(b)]. It is remarkable that for Gaussian arrays there occur no significant additional antipeaks due to a partially coherent superposition of the array junction currents.

In general, the necessary conditions for a generic unconventional array described in Sec. III are not sufficient to achieve a voltage response function for which all additional significant antipeaks due to a partially coherent superposition of the array junction currents disappear totally. By investigating several different unconventional gratings and the corresponding structure factors we observed, that for some area distributions additional antipeaks with voltage swings that are not much smaller than the voltage swings for totally coherent superposition do occur in the voltage response function. Their number decreases with increasing number of array loops. However, up to now, we did not find a direct link between the area size distribution of these arrays and the occurrence of the additional antipeaks. The problem is that

the number of combinations of array junction currents which can lead to a partially coherent superposition increases exponentially with increasing number of array loops. From the analytical results obtained for Gaussian arrays we feel that this problem, at least for some special configurations, may be solved using number theory. This point, however, needs further investigation.

### B. Inductive 1D parallel arrays

If the critical currents of the array junctions are not small or if the loop inductances are not negligible, i.e., if the inductance parameter  $\beta_L$  of the largest loop in the array becomes  $\beta_L \approx 1$  or larger, the self- and mutual inductances present in the array cannot be neglected and the Biot-Savart type inductive couplings among the currents flowing in the array need to be taken into account.

In this case the magnetic field  $\mathbf{B}$  in Eq. (6) is a superposition of the primary external magnetic field  $\mathbf{B}^{(1)}$  as generated by external sources, and the secondary magnetic field  $\mathbf{B}^{(2)}$ , which is induced by all currents flowing in the circuit

$$\mathbf{B} = \mathbf{B}^{(1)} + \mathbf{B}^{(2)}. \quad (20)$$

The currents flowing in the array are a superposition of the externally fixed bias current  $I$  which is, in general, not homogeneously distributed among the array junctions, and the array loop screening currents induced by the total magnetic field  $\mathbf{B}$ .

For current biased 1D parallel arrays, consisting of  $N-1$  loops and altogether  $N$  Josephson junctions there flow altogether  $N$  array junction currents. One of these junction currents, say  $I_N$ , may be determined in terms of the other  $N-1$  junction currents  $I_n$  using current conservation

$$I = \sum_{n=1}^N I_n. \quad (21)$$

The remaining  $N-1$  independent junction currents  $I_1, \dots, I_{N-1}$  constitute the  $N-1$  degrees of freedom of the system. They may be expressed, e.g., by using the RCSJ model, by the gauge invariant phase differences  $\varphi_1, \dots, \varphi_{N-1}$  at the corresponding Josephson junctions of the array.

Now, the secondary field  $\mathbf{B}^{(2)}$  generates a secondary magnetic flux  $\Phi_n^{(2)} = \langle \mathbf{B}^{(2)}, \mathbf{a}_n \rangle$  threading the area element  $\mathbf{a}_n$  of the array. With  $\mathcal{L}$  and  $\mathcal{M}$  denoting the inductance matrices of the array, the vector of secondary magnetic flux  $\Phi^{(2)} = (\Phi_1^{(2)}, \dots, \Phi_{N-1}^{(2)})$ , may be expressed in the form

$$\Phi^{(2)} = -\mathcal{L} \circ \mathbf{I} + \mathcal{M} \circ \mathbf{J}, \quad (22)$$

where  $\mathbf{I} = (I_1, \dots, I_{N-1})$  is a  $(N-1)$ -dimensional vector that represents the discrete current distribution within the array due to the  $N-1$  independent array junction currents, and  $\mathbf{J}$  is a vector which describes in what manner the bias current is fed into and extracted from the array. If the bias current  $I$  is fed into and out of the array in a homogeneous manner there simply holds  $\mathbf{J} = (I/N)(1, 1, \dots, 1)$ . However, if the bias current is fed into the array inhomogeneously, the

magnetic field generated by the bias current induces, possibly, additional flux into the loops of the array.

The inductance matrix  $\mathcal{L}$  may be interpreted as the ‘inductance’ matrix of the screening currents, while the matrix  $\mathcal{M}$  describes the redistribution of the bias current including the current enhancement at the array edges due to, in general nonsymmetric, Meissner screening effects. The inductance matrices  $\mathcal{L}$  and  $\mathcal{M}$  depend on the geometry of the network and also on the geometry of the current leads. They can be calculated using Ampère’s law. The coefficients  $L_{n,m}$  of  $\mathcal{L}$  (and analogously of  $\mathcal{M}$ ) can be computed from the coefficients  $L_{n,m}^*$  of the dual inductance matrix  $\mathcal{L}^*$ , as explained in greater detail, for example, in Refs. 12, 16–18. As a matter of fact, the inductive couplings among the loop currents  $I_n^*$  as given by the dual induction coefficients  $L_{n,m}^*$  may be expressed in terms of the  $N-1$  independent array junction currents  $I_1, \dots, I_{N-1}$ , since these currents span a basis of the  $(N-1)$ -dimensional state space of the current distribution. With  $\mathbf{I}^* = (I_1^*, \dots, I_{N-1}^*)$  denoting the corresponding vector of the eddy loop currents in the array one finds  $\mathbf{I}^* = \mathcal{T} \circ \mathbf{I}$ , where  $\mathcal{T}$  is a linear (dual) transformation connecting  $\mathbf{I} = (I_1, \dots, I_{N-1})$  with  $\mathbf{I}^*$ . So,  $\mathcal{L}$  is connected to  $\mathcal{L}^*$  by  $\mathcal{L} = \mathcal{L}^* \circ \mathcal{T}$ .

Defining the state vector of the  $N$  network variables by  $\varphi = (\varphi_1, \dots, \varphi_N)$ , we rewrite the condition of flux quantization, Eq. (6), using obvious notation in matrix form

$$\mathcal{N} \varphi = \frac{2\pi}{\phi_0} (\Phi^{(1)} + \Phi^{(2)}), \quad (23)$$

where  $\Phi^{(1)} = (\langle \mathbf{B}^{(1)}, \mathbf{a}_1 \rangle, \dots, \langle \mathbf{B}^{(1)}, \mathbf{a}_{N-1} \rangle)$  denotes the vector of primary magnetic flux. In Eq. (23) the network matrix  $\mathcal{N}$  represents the distribution of the Josephson junctions within the array. For our 1D parallel junction arrays  $\mathcal{N}$  is a di-diagonal  $(N-1) \times N$  rectangular matrix with nonvanishing elements  $\mathcal{N}_{n,m}$  given by  $\mathcal{N}_{n,n} = -1$  and  $\mathcal{N}_{n,n+1} = 1$  [see Eq. (6)].

Using the RCSJ model [see Eq. (2)], the system of coupled network equations for the phase variables  $\varphi_n(t)$  in the array can be stated, for  $n=1, \dots, N$ , in the form of a coupled nonlinear system of differential equations

$$\sin[\varphi_n(t)] + T_N(RC \partial_t^2 + \partial_t) \varphi_n(t) = \frac{I_n(\varphi)}{I_c}, \quad (24)$$

where, for simplicity, we have assumed identical array junction parameters. For  $n=1, \dots, N-1$  the right hand side  $I_n(\varphi)$  denotes the corresponding component of the vector  $\mathbf{I}(\varphi)$  of array junction currents, which follows combining Eqs. (22) and (23) in terms of the matrix inverse of  $\mathcal{L}$  in the form

$$\mathbf{I}(\varphi) = \mathcal{L}^{-1} \circ \mathcal{M} \circ \mathbf{J} + \mathcal{L}^{-1} \circ \left[ \Phi^{(1)} - \frac{\Phi_0}{2\pi} \mathcal{N} \varphi \right]. \quad (25)$$

For the last component,  $n=N$ , we find

$$I_N(\varphi) = I - \sum_{n=1}^{N-1} I_n(\varphi) \quad (26)$$

using Eq. (21).

In the continuum limit, i.e., sending the areas of the array loops to zero while the lateral length of the configuration persists, Eq. (24) describes a single so called (one-dimensional) *long* Josephson junction. In this case  $\varphi_n(t)$  transforms according to  $\varphi_n(t) \rightarrow \varphi(x_n, t) \rightarrow \varphi(x, t)$  with  $\varphi(x, t)$  denoting the gauge invariant phase difference across the extended junction, and  $x$  denoting the coordinate along the extended barrier. Equation (24) is then comparable with the standard continuum Ferrel-Prange equation<sup>19</sup> (also known as the sine-Gordon model<sup>20</sup>). However, there are two main differences between the sine-Gordon model and our model. (i) The sine-Gordon model cannot be used to describe *nonperiodic* structures. (ii) In order to compute solutions of the sine-Gordon equation, the boundary conditions and the initial current density distribution of the bias current have to be introduced by hand. For our model this is not the case. The solutions of Eq. (24) automatically satisfy all boundary conditions. In particular, the effects of the ‘discrete’ Meissner screening in the array are automatically taken into account in our calculations.

For the 1D parallel arrays with *unconventional grating structure* under consideration we computed the inductance matrices  $\mathcal{L}$  and  $\mathcal{M}$  assuming an array geometry similar to that shown in Fig. 1(c), i.e., a thin film geometry with superconducting leads with rectangular cross section. Also, we restricted to homogeneous feeding of the bias current. The kinetic inductance<sup>21</sup> of the currents flowing in the interior of the superconducting leads was taken into account by computing for a finite magnetic penetration depth and a fixed typical value of the current the current density within the leads. Then we took the linear approximation of this current density and used the corresponding current density profile for the computation of the inductance matrices. Changing the geometry of the network leads or the current density profile within the leads, did not give significant variations in our results if the arrangement of the array junctions within the leads is not generating strong asymmetries in the current density.

By numerically integrating the network Eq. (24) we computed the voltage response function  $\langle V_{xy} \rangle$  of various parallel junction arrays with unconventional grating structures, and this for weak, medium and strong inductive couplings. In order to allow a direct comparison with a two junction SQUID we use the parameter  $\beta_L$ , i.e., the inductance parameter of the largest area element  $\mathbf{a}_L$ , as a dimensionless measure for the inductance of the array. In all cases we observed, that **the qualitative behavior of the voltage response  $\langle V_{xy} \rangle$  does not get affected by the presence of inductive couplings.** In particular, the periodicity properties of the voltage response  $\langle V_{xy} \rangle$  and the characteristic interference properties around zero field are preserved. Also, additional significant antipeaks due to a partially coherent superposition of the array junction currents do not occur. This can be understood by the fact that the inductance matrix  $\mathcal{L}$  is a function of the geometry of the array, because it is the geometry (together with the London equations describing the penetration of field

into the individual superconducting wires) that governs the spatial current distribution. Therefore, there exists an implicit relation between  $\mathcal{L}$  and the structure factor  $S_N$  of the array. While the details of the voltage response are governed by  $\mathcal{L}$ , it turns out that the structure factor concept introduced in Sec. IV A is very helpful to characterize the basic interference properties of different array configurations without the need of (extended) numerical computations.

In order to exemplify the effects of finite array inductance we again use the Gaussian array. Figure 2 shows the voltage response  $\langle V_{xy} \rangle$  vs external flux  $\Phi^{(1)}$  threading the largest area element  $\mathbf{a}_L$  of the Gaussian array for various inductive couplings in the limit of vanishing capacitance, i.e.,  $C=0$ . Both the antipeak at  $\Phi^{(1)}=0$ , and the long periodicity of such arrays are preserved for finite inductive coupling. As  $\beta_L$  increases, the difference  $\max\langle V_{xy} \rangle - \min\langle V_{xy} \rangle$  (and therewith the transfer factor  $V_\Phi$ ) decreases. If the inductive couplings are not too strong the linewidth of the minimum  $\langle V_{xy} \rangle$  around  $\Phi^{(1)}=0$  scales proportional to  $1/N$ . Also for finite inductive coupling (and constant bias current  $I$ ) the voltage response  $\langle V_{xy} \rangle$  shows an asymmetry under  $\Phi^{(1)} \rightarrow -\Phi^{(1)}$ . This asymmetry is due to the asymmetry of the magnetic self-field generated by the bias current. In practice, however, this self-field can be suppressed by using the method of bias reversal.<sup>4</sup> For underdamped array junctions the voltage response function shows a number of additional features which will be discussed elsewhere.<sup>22</sup>

As far as disorder is concerned, we find that the voltage response  $\langle V_{xy} \rangle$  of Gaussian arrays is very responsive to adding small random fluctuations to the size distribution of the area elements, so that  $\langle V_{xy} \rangle$  becomes nonperiodic, and displays a pronounced antipeak only around  $\Phi^{(1)}=0$ . All other periodic antipeaks for finite external magnetic field disappear completely if the sum of the random size fluctuations approaches the size of the smallest loop in the array  $|\mathbf{a}_1|$ . In this case a Gaussian array becomes a generic unconventional array.

This scenario is different for periodic arrays. If we perturb the area sizes starting from a periodic array, we find for small perturbations, i.e., the sum of the size fluctuations is much smaller than  $|\mathbf{a}_L|$ , that the periodic antipeak pattern of a periodic grating [see Fig. 1(b)] gets actually modulated by the aperiodic grating pattern defined by the size fluctuations. So, the pattern is characterized by  $\Phi_0$ -periodic antipeaks with different voltage swings. For increasing amplitude of the size perturbations some of the antipeaks disappear in an irregular manner. It is clear, that for large perturbations, i.e., if the sum of the size fluctuations is comparable to  $|\mathbf{a}_L|$ , we finally end up with a generic unconventional grating structure, too.

## V. NOISE PROPERTIES

In view of applications, we briefly discuss in this section the energy resolution, i.e., the sensitivity, of magnetometers based on 1D parallel junction arrays with unconventional grating structures. As a starting point we recall the discussion presented in Ref. 4 for a conventional SQUID. Assum-

ing uncorrelated Nyquist noise sources located at the individual Josephson junctions, e.g., for shunted junctions at the shunt resistors, for frequencies  $f$  of the noise sources well below the Josephson frequency  $\nu_B$ , the currents flowing through a single junction produce a white voltage noise with spectral density  $s_V(f)$ . With  $v_\Phi$  denoting the transfer function of a single two-junction SQUID, the noise energy per unit bandwidth can be expressed as

$$\epsilon_0(f) = \frac{s_V(f)}{2 L v_\Phi^2}, \quad (27)$$

where  $L$  is the inductance of the single SQUID loop.<sup>4</sup> Consider now a periodic array with  $N$  junctions for which each array loop has an inductance of  $L$  and for which the inductive couplings between different array cells are not too strong. These inductive couplings depend on the geometry of the array. For the ladderlike array of Fig. 1(b) the intercell couplings are not negligible. However, it is clear that array geometries can be found for which the intercell couplings are substantially reduced, while the functional array grating is preserved. If  $N$  is the number of array junctions, the voltage noise of such an array scales with  $\sqrt{N}$ , since the noise sources are uncorrelated. The spectral density of the voltage noise  $S_V(f)$  of the array therefore scales with  $N$ . The voltage transfer function  $V_\Phi$  of the array also scales with  $N$ . This scaling behavior can be directly determined by solving the transcendental equations following from Eqs. (14) and (15) for  $\partial V/\partial \Phi$  and  $\partial^2 V/\partial \Phi^2$ . Now, combining the scaling behavior of the voltage noise and the scaling behavior of the transfer function leads for the noise energy of the periodic array  $\epsilon(f)$  to the expression

$$\epsilon(f) = \frac{1}{N} \alpha \epsilon_0(f), \quad (28)$$

where  $\alpha$  is a constant proportionality factor depending on inductive intercell couplings. The noise energy from Nyquist noise therefore scales for a periodic array with  $1/N$ . This scaling behavior does not change for unconventional grating structures. If the loop sizes of the array loops are different, i.e.,  $L_i \neq L_j$ , only the constant proportionality factor  $\alpha$  in Eq. (28) changes, since  $\alpha$  depends on the structure factor  $S_N^{(\Phi)}$  of the unconventional array. The scaling behavior of the voltage transfer function  $V_\Phi$  is independent of the particular structure factor.

This concludes our discussion of the noise properties of unconventional arrays with respect to white voltage noise. In Sec. VI we will discuss possible advantages of unconventional arrays with respect to other noise sources, i.e.,  $1/f$  noise by moving flux vortices.

## VI. DISCUSSION

We have shown that parallel 1D arrays of Josephson junctions with unconventional grating structures may have properties that differ significantly from those of conventional configurations. Under certain conditions, the voltage response function of generic unconventional arrays becomes

nonperiodic with a pronounced antipeak only around  $\mathbf{B}=0$ . This property is shown to be directly related to the distribution of the array loop sizes and independent of spreads in the individual array junction parameters. For special unconventional grating structures the voltage response has a periodicity that is much larger than  $\Phi_0$ . It is shown that the period can be directly controlled by the loop size distribution without any loss of sensitivity. In view of applications of unconventional arrays as magnetometers the energy resolution of such devices is discussed. It is shown, that this energy resolution can be expected to increase substantially with increasing number of array junctions. With regard to white voltage noise, the scaling factor for the noise energy per unit bandwidth was determined to be  $1/N$ .

The theoretical description of unconventional grating structures developed in Sec. IV A, allows us, by means of the structure factor, to determine the basic qualitative interference properties of the voltage response analytically even in the case of inductive arrays. Therefore, the structure factor may be a very helpful tool to construct arrays with specific voltage response functions.

In presenting results, we have restricted ourselves on arrays with planar geometries for which the orientated area elements  $\mathbf{a}_n$  all possess the same orientation. However, the structure factor concept introduced in Sec. IV A applies quite generally also for arrays for which the area elements have different orientation. In particular, if a vector basis of the three-dimensional space can be generated from the set  $\{\mathbf{a}_n\}$ , the 1D array becomes sensitive to the *orientation* of the external magnetic field. By measuring the control currents flowing through a set of suitably orientated compensation coils, this would allow the *absolute* measurement of all three cartesian components of an external magnetic field.

The problem of additional antipeaks in the voltage response function due to a partially coherent superposition of the array junction currents is still open. As discussed in Sec. IV, we found some grating structures for which such additional antipeaks appear even for large  $N$ . This feature may be connected to some (hidden) quasi-periodicity of the structure factor and may be solved using number theory. Also, the Gaussian array which was used to exemplify the effects of unconventional grating has some remarkable additional features which are connected to number theory. All of these features, however, need further investigation.

The noise properties of unconventional gratings discussed in Sec. V indicate that, at least for low- $T_c$  devices, magnetometers based on the 1D parallel arrays may have a very high sensitivity without being much complicated to fabricate. Together with the uniqueness of the voltage response function this property may be suitable to design robust and reliable superconducting electronic devices of different kind.

In addition to the white noise discussed in Sec. V, the noise properties of high-transition-temperature SQUID's are often determined by low frequency  $1/f$  noise generated by moving flux vortices trapped in the superconducting bulk material from which the devices are built up. In particular, if additional bulk material is used to focus the flux induced by an external magnetic field into the SQUID loop this  $1/f$  noise increases substantially because of the large number of

trapped vortices. Unconventional grating structures may help to solve this problem. In order to achieve the same magnetic field resolution as, e.g., a conventional high- $T_c$  SQUID's with washer design,<sup>4</sup> for an array much less superconducting bulk material is needed. This strongly reduces the number of trapped flux vortices. In addition, due to inhomogeneities in the superconducting bulk material, the motion of these vortices is at most only partially correlated. Therefore, the above used argument concerning the summation of voltage noise generated by uncorrelated noise sources should also hold for the flux noise produced by uncorrelated moving flux vortices. Therefore, the signal to noise ratio can be expected to increase with increasing number of array loops, even if moving flux vortices are present.

In view of high- $T_c$  devices, another advantage may be that the requirements on unconventional grating structures with respect to the spread of the junction parameters and the loop sizes are low. From our discussion in Sec. IV A it can be inferred that **the performance of the device is determined by the mean values of the junction parameters only. Even large parameter spreads should not influence proper operation.** This claim was confirmed by various numerical simulations with different structure factors and different parameter spreads. If the unconventional array is designed such that the voltage response function antipeak at  $\mathbf{B}=0$  is unique, deviations in the sizes of the loops are not critical (see Sec. IV B). This situation is different for periodic arrays.

Periodic arrays do not possess any kind of structural stability. If the loop sizes are not perfectly identical, the response function shows an irregular periodicity with antipeaks of different voltage swing. In practice, it can therefore not be expected that periodic arrays possess a suitable mode of operation.

Based on our theoretical work, together with Träuble we recently started to carry out first experiments on arrays with unconventional grating structures. The experimental results up to now confirm our theoretical predictions concerning the magnetic field dependence of the voltage response function very well.<sup>23</sup> However, additional experiments have to be carried out and the noise properties have to be measured.

To conclude with regard to applications, magnetometers based on 1D parallel Josephson junction arrays with unconventional grating structures may stimulate the development of new types of robust superconducting quantum interferometers, which, e.g., would allow a technically rather simple precision measurement of *absolute* strength of magnetic fields.

#### ACKNOWLEDGMENTS

We thank R. P. Huebener, R. Kleiner, and T. Träuble for useful discussions. Support by ‘‘Forschungsschwerpunktprogramm des Landes Baden-Württemberg’’ is gratefully acknowledged.

- 
- <sup>1</sup>B.D. Josephson, *Phys. Lett.* **1**, 251 (1962).  
<sup>2</sup>T. Imamura and S. Hasuo, *J. Appl. Phys.* **39**, 280 (1988).  
<sup>3</sup>R. Gross, in *Interfaces in Superconducting Systems*, edited by S. L. Shinde and D. Rudman (Springer, New York, 1994), pp. 176-209.  
<sup>4</sup>D. Koelle, R. Kleiner, F. Ludwig, E. Dantsker, and J. Clarke, *Rev. Mod. Phys.* **71**, 631 (1999).  
<sup>5</sup>K.K. Likharev, in *Dynamics of Josephson Junctions and Circuits* (Gordon and Breach, New York, 1991).  
<sup>6</sup>I.K. Yanson, V.M. Svistunov, and I.M. Dmitrenko, *Zh. Éksp. Teor. Fiz.* **48**, 976 (1965) [*Sov. Phys. JETP* **21**, 650 (1965)].  
<sup>7</sup>F. London, in *Superfluids* (Dover, New York, 1961), Vol. I.  
<sup>8</sup>L. Onsager, *Nuovo Cimento* **6**, Suppl. 2, 249 (1949).  
<sup>9</sup>J. Clarke, in *Superconducting Devices*, edited by S. T. Ruggiero and D. A. Rudman (Academic, New York, 1990).  
<sup>10</sup>M. Tinkham, in *Introduction to Superconductivity*, 2nd ed. (McGraw-Hill, New York, 1996).  
<sup>11</sup>A.Th.A.M. de Waele, W.H. Kraan, and R. de Bruyn Ouboter, *Physica* (Amsterdam) **40**, 302 (1968).  
<sup>12</sup>D. Dominguez and J.V. José, *Phys. Rev. B* **53**, 11 692 (1996).  
<sup>13</sup>J. Oppenländer, Ch. Häussler, and N. Schopohl, *J. Appl. Phys.* **86**, 5775 (1999).  
<sup>14</sup>E. Lindelöf, in *Le Calcul des Résidues et ses Applications à la Théorie des Fonctions* (Chelsea, Paris, 1947).  
<sup>15</sup>M.R. Schröder, in *Number Theory in Science and Communication*, 3rd ed. (Springer, Berlin, 1999).  
<sup>16</sup>J.R. Phillips, H.S.J. van der Zant, J. White, and T.P. Orlando, *Phys. Rev. B* **47**, 5219 (1993).  
<sup>17</sup>D. Reinel, W. Dieterich, and T. Wolf, *Phys. Rev. B* **49**, 9118 (1994).  
<sup>18</sup>A. Tuohimaa, J. Paasi, T. Tarhasaari, T. Di Matteo, and R. De Luca, *Phys. Rev. B* **61**, 9711 (2000).  
<sup>19</sup>P.G. de Gennes, in *Superconductivity of Metals and Alloys* (Addison-Wesley, New York, 1989).  
<sup>20</sup>Y. Kivshar and B. Malomed, *Rev. Mod. Phys.* **61**, 763 (1989).  
<sup>21</sup>G. Hildebrandt and F.H. Uhlmann, *IEEE Trans. Appl. Supercond.* **5**, 2766 (1995).  
<sup>22</sup>J. Oppenländer, Ch. Häussler, and N. Schopohl (unpublished).  
<sup>23</sup>J. Oppenländer, T. Träuble, Ch. Häussler, and N. Schopohl, *IEEE Trans. Appl. Supercond.* (to be published March 2001).